Palaeogeography, Palaeoclimatology, Palaeoecology 468 (2017) 314–326

Contents lists available at ScienceDirect

Palaeogeography, Palaeoclimatology, Palaeoecology

journal homepage: www.elsevier.com/locate/palaeo

Turpanopitys taoshuyuanense gen. et sp. nov., a novel woody branch discovered in Early Triassic deposits of the Turpan Basin, Northwest China, and its palaeoecological and palaeoclimate implications

Xiao Shi [a,b,c], Jianxin Yu [a,b,*], Jean Broutin [c], Denise Pons [c], Camille Rossignol [d,e], Sylvie Bourquin [d], Sylvie Crasquin [c], Qiang Li [a,b], Wenchao Shu [a,b]

[a] State Key Laboratory of Biogeology and Environmental Geology, Wuhan 430074, China
[b] School of Earth Sciences, China University of Geosciences, Wuhan 430074, China
[c] Sorbonne Universités, CR2P-UPMC Paris 6-MNHN-CNRS, 75005 Paris, France
[d] Géosciences Rennes UMR CNRS 6118, Université Rennes 1, 35042 Rennes cedex, France
[e] Géohydrosystèmes Continentaux, EA 6293, Université François Rabelais, 37200 Tours, France

ARTICLE INFO

Article history:
Received 27 July 2016
Received in revised form 15 December 2016
Accepted 19 December 2016
Available online 21 December 2016

Keywords:
Turpanopitys taoshuyuanense gen. et sp. nov.
Palaeoecology
Palaeobiogeographic distribution
Early Triassic
Turpan Basin

ABSTRACT

A novel well-preserved woody branch, *Turpanopitys taoshuyuanense* gen. et sp. nov. was collected in the early Triassic terrestrial deposits in the Turpan Basin, Northwest China. The permineralized wood is characterized by a heterogeneous pith, endarch primary xylem and *Protophyllocladoxylon*-type secondary xylem. The pith consists of parenchyma cells and supporting diaphragms formed by brick-like sclerenchyma cells. The quantitative growth-ring analyses of *T. taoshuyuanense* indicate that the species was evergreen, the leaf longevity being comprised between 3 and 15 years. *T. taoshuyuanense* might indicate a warm humid climate with short dry periods in the Turpan basin in the Early Triassic. The *Protophyllocladoxylon*-type woods were widely distributed in different climate zone in both southern and northern hemispheres during the Palaeozoic and Early Triassic. The growth rings of the woods with *Protophyllocladoxylon*-type secondary xylem are good indicator for the palaeoclimate. The new specimen indicates that a warm humid climate with irregularly distributed short dry periods in the Early Triassic Turpan basin.

1. Introduction

Five mass extinctions were recognized in the Phanerozoic in animal families (Jablonski, 1985), while only two major extinctions could be clearly recognized in plant families (Cascales-Miñana and Cleal, 2013). The end-Permian mass extinction is the only one affecting conjointly terrestrial ecosystems (including plants) and marine ecosystems (Twitchett et al., 2001; Cascales-Miñana and Cleal, 2013). Based on the palaeobotanical data for the end-Permian from Northern China Block, several environmental stresses that affected end Permian terrestrial ecosystems were identified, for instance, wind activity, fungal proliferation, water stress, elevated atmospheric CO_2 concentration and wildfire (Wang and Zhang, 1998). After this severest extinction, the physical environments remained very disturbed during the next 5–6 Myr (Retallack et al., 2011; Chen and Benton, 2012; Sun et al., 2012; Retallack, 2013; Benton and Newell, 2014). As a result, plant diversity did not return to the pre-extinction levels until the Late Triassic (Chen and Benton, 2012).

The reconstruction of palaeoenvironmental conditions prevailing during the end Permian mass extinction and subsequent Triassic recovery is essential to better constrain the potential causes and mechanisms that lead to this major biotic turnover. Anatomical features observed from fossils, including plants, provide key palaeoecologic and palaeoclimatic information (e.g., Royer et al., 2005; Knoll et al., 2007). In this paper, we describe a new woody branch discovered in the transitional Permian-Triassic deposits of the Guodikeng Formation in the Turpan Basin, Northwest China. The results of a quantitative growth-ring analysis are good enough to give accurate palaeoecological interpretations. A bibliographical survey allowed us to analyse the palaeogeographic distribution of *Protophyllocladoxylon*-type woods during late Palaeozoic.

2. Geological setting, materials, and methods

The Turpan Basin, located in the Xinjiang Uygur autonomous Province, northwest China (Fig. 1), covers about 53, 500 km^2, and constitutes the third lowest exposed terrestrial point on the earth's surface.

* Corresponding author at: State Key Laboratory of Biogeology and Environmental Geology, Wuhan 430074, China.
E-mail address: yujianxin@cug.edu.cn (J. Yu).

http://dx.doi.org/10.1016/j.palaeo.2016.12.026
0031-0182/

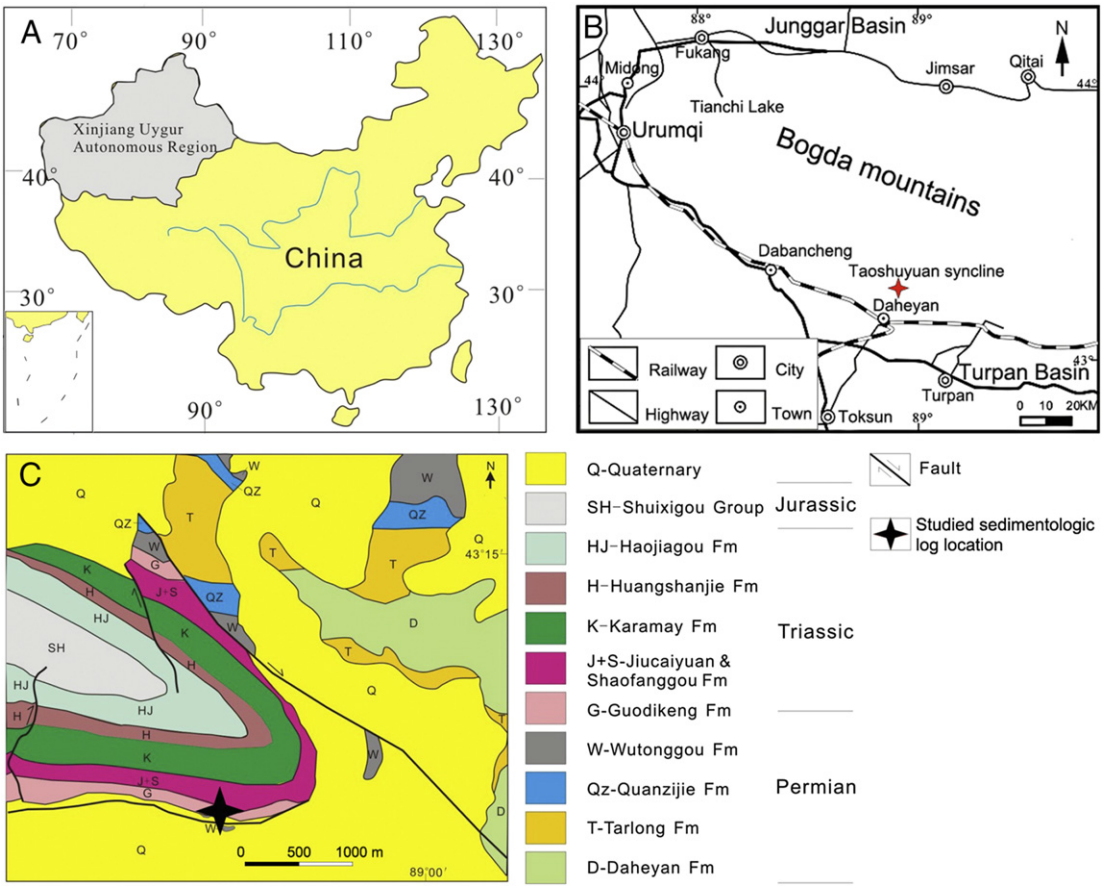

Fig. 1. (A) Location of Xinjiang Uygur Autonomous Region. (B) Location of the Taoshuyuan anticline. (C) Geological map of the Taoshuyuan syncline.

The present boundaries of the basin are the Bogda and Haerlike Mountains to the north and the Juluotage Mountains to the south. During the Late Permian to the Early Triassic, the basin was located on the Junggar block that constituted a part of the Pangea supercontinent (e.g., Domeier and Torsvik, 2014; Fig. 2). The Turpan Basin was further located on the northwest coast of a Palaeotethys branch (Fig. 2) that progressively disappeared as a result of a northwestward subduction (e.g., Xiao et al., 2009). The Turpan Basin consequently migrated northward from 40 to 50°N palaeo-latitude during Kungurian–Wuchiapingian time (McElhinny et al., 1981; Sengor and Nat'lin, 1996; Ziegler et al., 1997; Scotese, 2001; Yang et al., 2010). Late Permian to Early Triassic deposits mainly correspond to alluvial and lacustrine settings (e.g., Greene et al., 2005) emplaced in many small grabens and half grabens (Allen et al., 1995; Sengor and Nat'lin, 1996; Yang et al., 2007, 2010).

The Taoshuyuan section is located on northern side of the Turpan Basin, in the foothill of the Bogda Mountains (Fig. 1). The section crops out on the southern flank of a WNW-ESE trending axial plan syncline (Fig. 1C). The lithostratigraphy, biostratigraphy and cyclostratigraphy of this area are well established (Zhang, 1981; Liao et al., 1987; Cheng et al., 1996; Wartes et al., 2002; Zhu et al., 2005; Yang et al., 2007, 2010).

The specimen was collected from the Guodikeng Formation in the southern limb of Taoshuyuan syncline (GPS: 43° 57′ 59.6″ N, 88° 52′ 02.2″ E; Fig. 1C). The fossil plants, spores and pollen assemblages, palaeomagnetism and $\delta^{13}C_{org}$ data suggest the Permian-Triassic boundary within 61–66 m below the basalmost deposits of the Jiucaiyuan Formation in the northern limb of the Taoshuyuan syncline (Sun, 1989; Li et al., 2004; Cao et al., 2008; Liu, 2000). The sample has been found in fine-grained sandstone deposits, 25 m below the basalmost beds of Jiucaiyuan Formation, with current and wave ripples, attributed to coastal lake environment (Fig. 3). In the silty clay level above the bed where we collected the wood specimen, Cheng et al. (1996) found fossils of vertebrate *Lystrosaurus* (Fig. 3). *Lystrosaurus* is classically considered as an Early Triassic marker (succeeding to the Permian *Dicynodon*, e.g., Lucas, 1998; Lucas, 2009). In consequence, the upper part of the Guodikeng Formation is traditionally considered as Early Triassic in age (Fig. 3). However, a stratigraphic overlap of *Dicynodon* and *Lystrosaurus* has been documented in the closely located Junggar Basin (e.g., Metcalfe et al., 2009) as well as in other part of the world (e.g., Smith and Ward, 2001 for the Karoo Basin, South Africa). As a result, although the exact location of the Permian-Triassic boundary in this section is still unknown, the bed where we found the specimen can be considered as Early Triassic in age.

To investigate the wood fossils, thin-sections were made using conventional cutting and polishing methods for optical microscopic observations. Slides were photographed with Panasonic a DMC-FZ28 digital camera. The anatomy of the wood was studied using a microscope Leica DM4000B. Photomicrographs were taken with Nikon D300 digital camera. Images in plates are basically processed and stitched together by Adobe Photoshop CS v. 6. All the specimens and slides are housed in the State Key Laboratory of Biogeology and Environmental Geology, China University of Geosciences (Wuhan), under catalogue number: XTT–C–4.

To infer intraseasonal conditions and leaf longevity patterns of the tree, Falcon-Lang (2000a) developed the CSDM curve (Cumulative Sum of the Deviation from Mean diameter).

We selected five adjacent growth rings and measured the radial diameter of five adjacent rows of cells for each growth ring to construct the CSDM curve. The radial diameters of the cells were then averaged using the method of Falcon-Lang (1999).

3. Systematic palaeontology

CLASS Coniferopsida Sternberg, 1820
ORDER Coniferophyte Sternberg, 1820

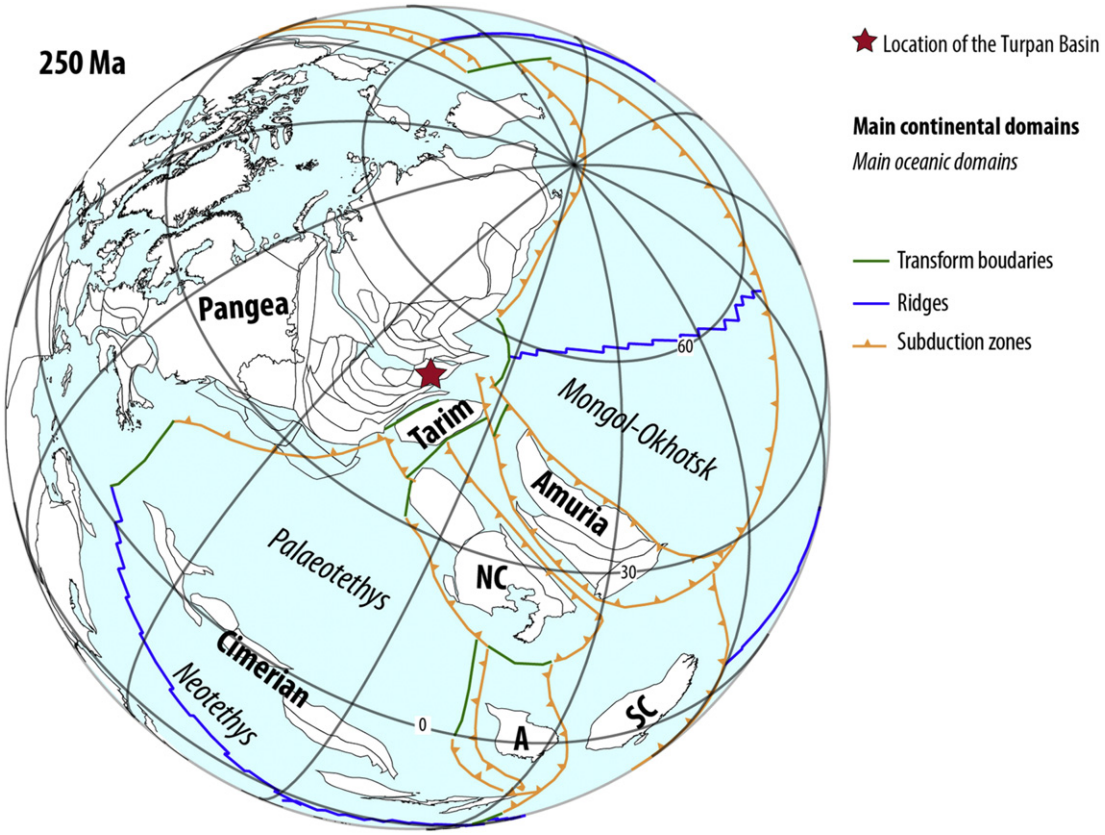

Fig. 2. Simplified palaeogeographic reconstruction showing the location of the Turpan Basin at 250 Ma. A: Anamia; NC: North China block; SC: South China block. Modified after Domeier and Torsvik, 2014. Reconstruction generated using GPlates software (http://gplates.org).

FAMILY Incertae sedis

GENUS *Turpanopitys* gen. nov. Shi, Yu, Broutin and Pons

Genus diagnosis: pith heterogeneous with parenchyma cells and supporting diaphragms. Primary xylem endarch. Tracheids in primary xylem with annular, helical and reticulate thickenings. Secondary xylem homoxylic. Tracheids with araucarian radial pitting. Xylem rays homogeneous. Cross-fields with simple pits. Vertical parenchyma cells and secretory cells absent.

Etymology: the generic name is derived from the Turpan Basin, where the type specimen was collected.

Holotype: *Turpanopitys taoshuyuanense* gen. et sp. nov. Shi, Yu, Broutin and Pons

Repository: State Key Laboratory of Biogeology and Environmental Geology, China University of Geosciences (Wuhan), Wuhan, China.

Type locality: Taoshuyuan, Turpan, Xinjiang Uygur Autonomous Region, PR China. (Fig. 1)

Stratigraphic horizon and age: upper part of Guodikeng Formation, Early Triassic.

Etymology: the specific name is derived from the Taoshuyuan syncline, where the type specimen was collected.

Type species: *Turpanopitys taoshuyuanense* gen. et sp. nov. Shi, Yu, Broutin and Pons

Specific diagnosis: pith heterogeneous with parenchyma cells and supporting diaphragms. Diaphragms consist of brick-like sclerenchyma cells. Sclerenchyma cells vertically regularly aligned. Primary xylem endarch. Tracheids in primary xylem with annular, helical and reticulate thickenings. Secondary xylem homoxylic, with indistinct growth rings. Tracheids with uni- to triseriate araucarian pits. Xylem rays uniseriate (rarely biseriate), homogeneous, 1–40 cells high. Cross-fields with 1 (up to 3), rectangular, oval or round, simple, sometimes slightly areolate pits. Vertical parenchyma cells and secretory cells absent.

4. Description

The calcified fossil wood piece is about 12.5 cm long with a maximum diameter of 9.0 cm (Fig. 4A). Interestingly, a young lateral branchlet emerges horizontally from the main branch (Fig. 4B, C). No cortical tissues are preserved. The pith was preserved only in the branchlet. In the branch, it was impossible to get any slides of the pith. Several leaf traces, helically arranged, occur in the secondary xylem of the branchlet and cross the growth-ring boundary (Fig. 4C, E). This indicates that the species is evergreen (Falcon-Lang and Cantrill, 2001).

4.1. Pith

The pith is circular in outline. Along the direction of the branchlet extension, the pith diameter increases from 0.6 to 1.65 cm (L = 5.5 cm) (Fig. 5A). Two slides along the transversal direction and two slides along the radial direction were made. The pith of the branchlet is heterogeneous. It consists of parenchyma cells and diaphragms made of sclerenchyma-like cells. The parenchyma cells are isodiametric, circular or polygonal in transverse section, diameter 25 to 152.5 μm (Fig. 3D). The wall is mean 2.4 μm thick. Some cell walls are dark brown. Intercellular spaces are visible.

Seven complete diaphragms can be observed in the present specimen (Fig. 5A). In the radial section, the diaphragms are lense-like (Fig. 5A, B). Two perpendicular radial sections of the pith indicate that these diaphragms are true platforms (Fig. 5C, D). The intact diaphragms are horizontal or slightly curved, but three incomplete diaphragms at the top of the branchlet appear bent (Fig. 5A). Their thickness decreases gradually from the middle part of the pith to the periphery and reduces to one or two cells at the contact with the primary xylem or the initial secondary xylem (Fig. 5E, F). The middle part of the diaphragm is 0.32 to 1.24 mm thick and only one or two cells thick at the peripheral ends.

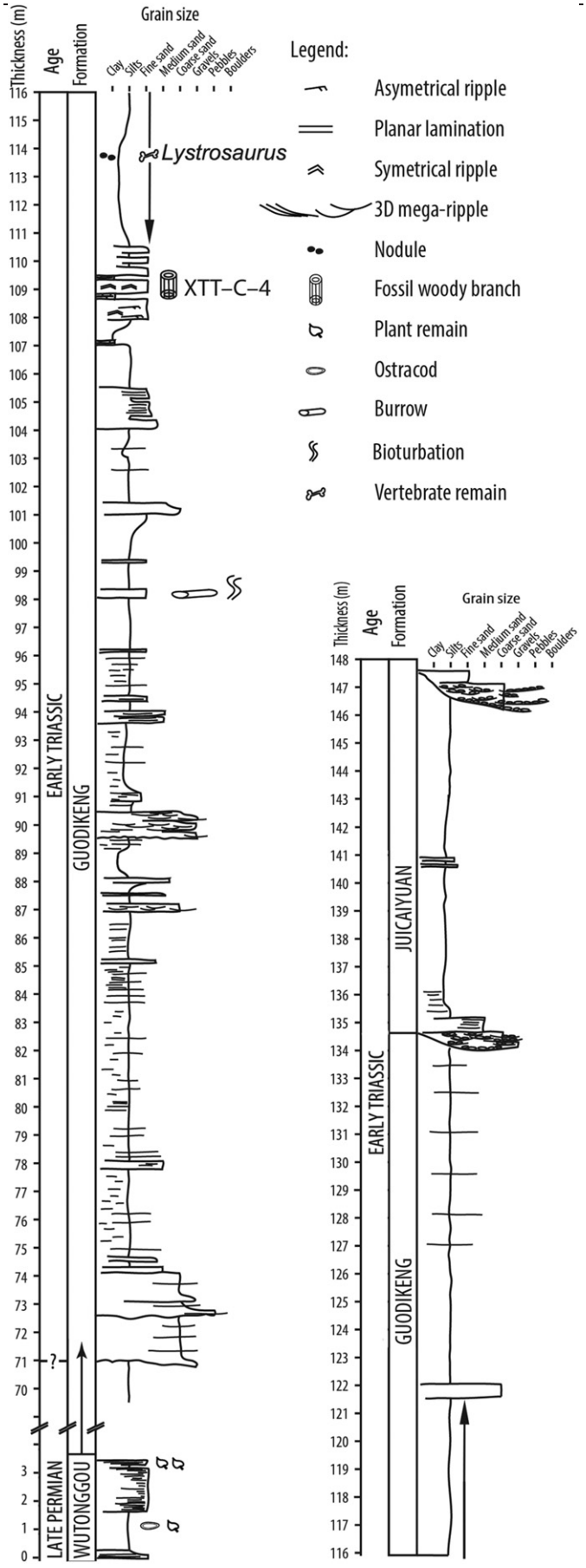

The sclerenchyma cells of the diaphragms are brick-like. In radial section, the sclerenchyma cells are very close and vertically regularly arranged in lines. The intercellular spaces are absent. The sclerenchyma cells are ca. 7.5 × 29 to 40 × 76 μm in size with 2.5 to 15 μm thick walls (Fig. 6A). The pith cells display lining-like structures inside the cell lumens and the cell walls are separated in some area. These artifact structures are caused by white rot.

4.2. Primary xylem

The primary xylem shows endarch maturation (Fig. 6B). The primary xylem tracheids are ca. 17.5 to 25 μm wide and show annular, helical and reticulate thickenings (Fig. 6C).

4.3. Secondary xylem

The secondary xylem is pycnoxylic, with tracheids and parenchymatous rays. Eight growth rings were preserved in the transverse section of the main branch (Fig. 6D). Early wood tracheids are circular or polygonal, while late wood ones are elliptical or rectangular. The percentage of late wood is 8.79–19.57%. The tracheids are 16 to 66 μm in diameter. The lumens of some tracheids are fully filled by tyloses.

In the radial section, pits on the tracheid walls are of araucarian type. In the branchlet, they are uniseriate (24%) or biseriate (74%), occasionally triseriate (2%) (Fig. 6E, F), while in the main branch, they are uniseriate (60%) or biseriate (40%) (Fig. 7A). When uniseriate, the pits are contiguous, circular or flattened, 5–15 μm from the tracheid internal walls, and the flattening index is 0.58–0.95; when biseriate or triseriate, the pits are alternate, crowded hexagonal, close to the internal wall of the tracheids, and the flattening index is 0.63–0.96. Near to the pith, some opposite pits can be observed (<1%). The pits are 7.5 to 20 μm in diameter, with circular or elliptical apertures.

Cross-field pits are rectangular, oval or round. They are simple, sometimes slightly areolate. In the branchlet, there is 1 or 2, rarely 3, pits in each cross-field unit (Fig. 7B, C). In the main branch there is only one pit in each cross-field unit (Fig. 7D). The pits are 9 × 12 μm to 28 × 35 μm (width × height).

The information for the tangential view is based only on the main branch. The lumens of tracheids are secondarily septate by numerous tyloses originating from ray cells (Fig. 7F). The homogeneous rays consist of elliptical or sub-rectangular parenchyma cells. The horizontal and tangential ray walls are smooth. They are uniseriate, or very rarely biseriate (<1%). Rays are constituted by 1–15 (>90%), up to 40, cells (30–1110 μm) high (Fig. 7E). There are 35 rays per square millimetre. Ray cells are 12.5 to 27.5 μm wide, and 17.5 to 32.5 μm high. Vertical parenchyma cells and secretory canals are absent.

5. Comparisons

The anatomical features of *Turpanopitys* gen. nov. closely resemble some extinct and extant conifers that also display a heterogeneous pith, endarch primary xylem and thick pycnoxylic secondary xylem. As the anatomy of the pith and primary xylem constitute critical criteria for the classification of gymnosperms woods (Lepekhina, 1972; Pant and Singh, 1987; Feng et al., 2011), we thus consider *Turpanopitys* gen. nov. as a coniferophyte of uncertain systematic affinity.

Turpanopitys gen. nov. possesses unique solid lenticular diaphragms in the pith. All the sclerenchyma cells of the diaphragms are morphologically different and smaller than the parenchyma cells and closely arranged without intercellular space. The sclerenchyma cell walls are thicker than that of parenchyma cell. Based on these characters, these diaphragms play clearly a role of support to the pith.

Fig. 3. Sedimentological section for the south limb of the Taoshuyuan syncline where the woody branch was found. Position of the sample is indicated (XTT-C-4). See Fig. 1C for location.

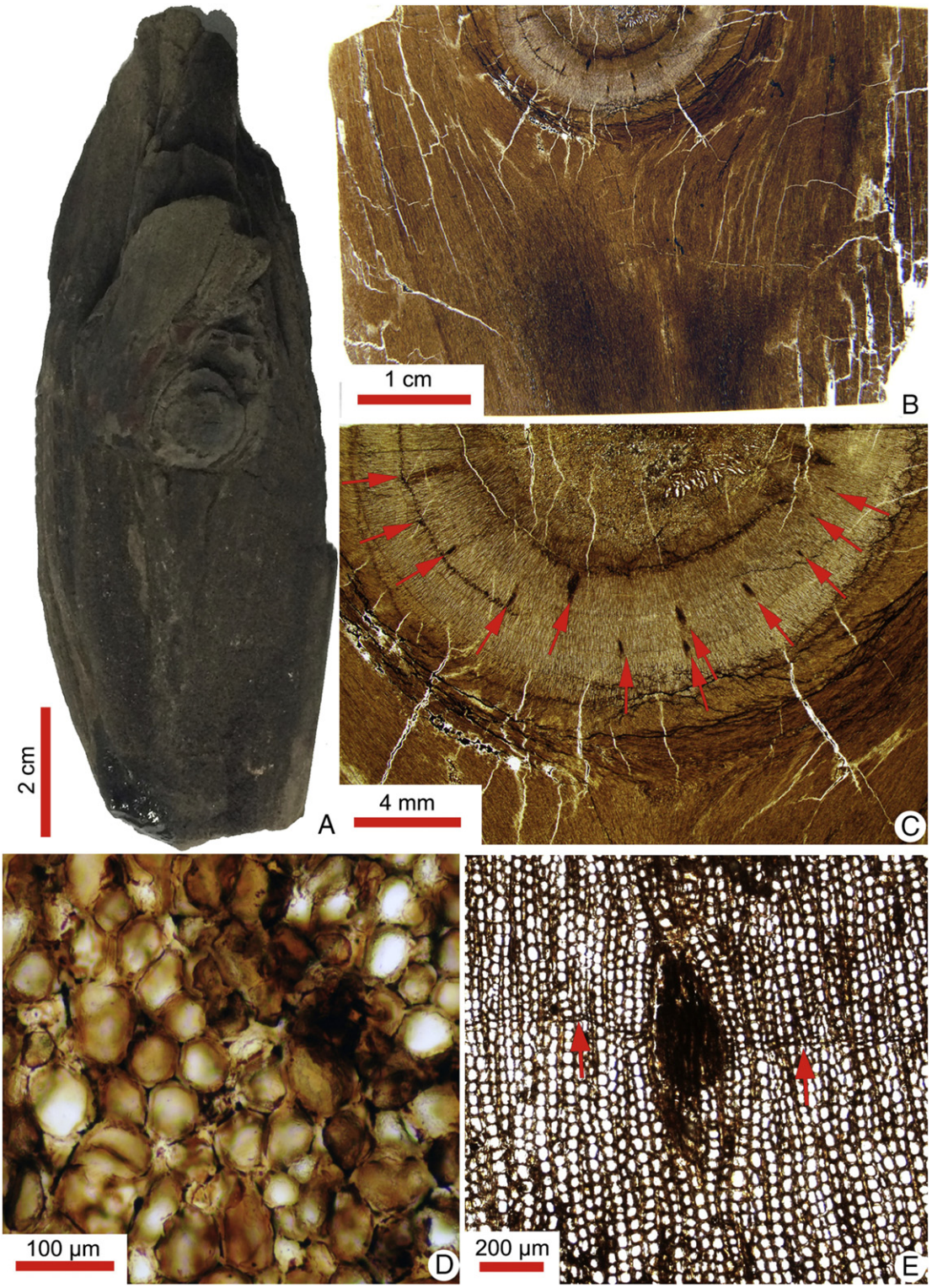

Fig. 4. *Turpanopitys taoshuyuanense* gen. et sp. nov. A. General view of the specimen XTT-*C*4. B. Overview of the pith and the primary xylem of the branchlet (transverse section) and the secondary xylem of the branch (tangential section). Slide number: XTT-C-4a1. C. Close-up of the pith with cracked cavities and the primary xylem of the branchlet (transverse section), red arrows: spirally arranged leaf traces. Slide number: XTT-C-4a1. D. Transverse section showing the isodiametric parenchyma cells in the pith. Slide number: XTT-C-4a1. E. Close up on a leaf trace across a growth-ring boundary (red arrows) in the secondary xylem. Slide number: XTT-C-4a1. (For interpretation of the references to colour in this figure legend, the reader is referred to the web version of this article.)

The secondary xylem of *Turpanopitys* gen. nov. is identical to *Protophyllocladoxylon* Kräusel: (1) presence of growth rings, (2) araucarian radial pitting of tracheids, (3) simple large oval or round cross-field pits, (4) absence of axial parenchyma and resin canals, (5) unpitted ray walls. About six morphogenera of fossil woods with a *Protophyllocladoxylon*-type secondary xylem and different structures of pith and primary xylem have been documented as far as we know from the Paleozoic and early-middle Triassic (Table 1). Among them, the pith of *Junggaropitys* Shi et al., 2015 is homogeneous that is different from *Turpanopitys* gen. nov.

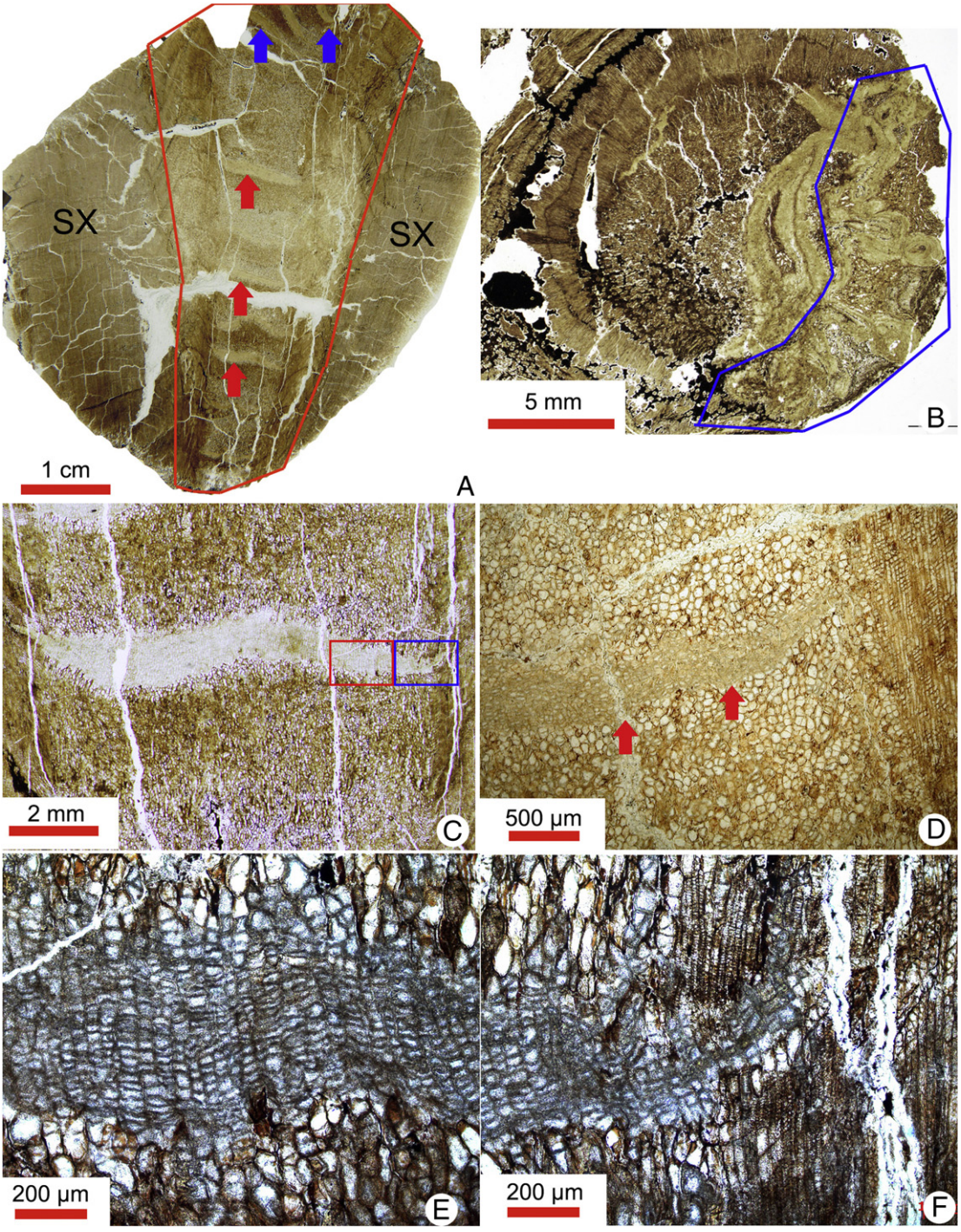

Fig. 5. *Turpanopitys taoshuyuanense* gen. et sp. nov. A. Overview of the pith and the primary xylem of the branchlet (radial section; in the red box) and the secondary xylem (SX) of the main branch (transverse section). The red arrows indicate the lense-like diaphragms and the blue arrows indicate the curved diaphragms in the pith. Slide number: XTT-C-4b1. B. Overview of the pith, primary xylem and secondary xylem of the branchlet (transverse section). The area in the blue box is disturbed due to a local maceration during decay. Slide number: XTT-C-4a2. C. Radial section showing one diaphragm in the pith. Slide number: XTT-C-4b1. D. Radial section showing one diaphragm (arrows) in the pith. Slide number: XTT-C-4b2. The slides XTT-C-4b1 and XTT-C-4b2 are perpendicular. E. Radial section showing the small brick-like supporting cells of the diaphragm (the red box in picture C). Slide number: XTT-C-4b1. F. Radial section showing the close-up of the diaphragm (the blue box in picture C). The thickness of the diaphragm reduces on the periphery of the pith. The diaphragm disappears at the contact with the initial of the secondary xylem. Slide number: XTT-C-4b1. (For interpretation of the references to colour in this figure legend, the reader is referred to the web version of this article.)

In some Late Palaeozoic coniferophytes related to the walchian Voltziales clade, sclerotic nests occur in the piths (e.g., *Barthelia*, *Emporia*, and *Hanskerpia* from the Upper Pennsylvanian of Hamilton Quarry, Kansas, U.S.A.; *Macdonaldodendron* from the Lower Permian and Upper Pennsylvanian, New Mexico, U.S.A.) (Rothwell and Mapes, 2001; Rothwell et al., 2005; Hernandez-Castillo et al., 2009a, 2009b, 2009c; Falcon-Lang et al., 2014, 2016). In most of these genera, the isolated sclerotic nests are irregularly distributed in the piths. But in Emporia, the sclerotic diaphragms occur as those in *Turpanopitys*. However, the secondary xylem of walchian conifer is characterized by predominantly uniseriate tracheid pitting and typically shows only one cupressoid pit per cross-field (Rothwell and Mapes, 2001; Rothwell et al., 2005; Hernandez-Castillo et al., 2009a, 2009b, 2009c; Falcon-Lang et al., 2014, 2016). That is different from the *Protophyllocladoxylon*-type secondary xylem in the new genus.

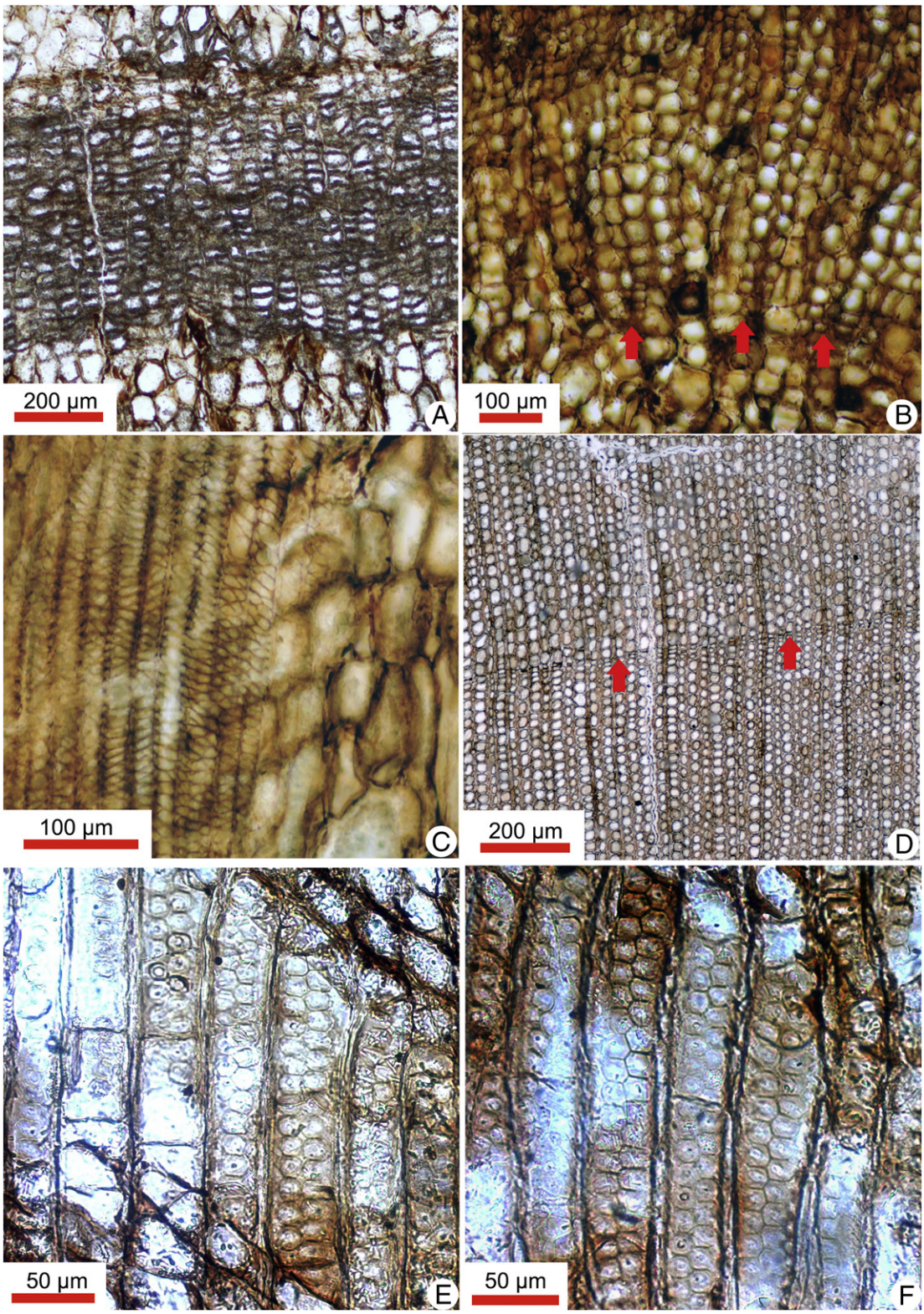

Fig. 6. *Turpanopitys taoshuyuanense* gen. et sp. nov. A. Close-up of the diaphragm cells. Slide number: XTT-C-4b1. B. Transverse section showing the endarch primary xylem (arrows) on the pith periphery. Slide number: XTT-C-4a1. C. Radial section showing the helical and reticulate thickenings of the tracheids of primary xylem. Slide number: XTT-C-4b1. D. Transverse section showing the subtle growth-ring boundary, characteristic of "indistinct growth rings" (arrows) in the secondary xylem of the main branch. Slide number: XTT-C-4b1. E, F. Radial section showing the uniseriate and biseriate radial pits on the tracheid walls in the branchlet. The biseriate pits are alternate or rarely opposite. Slide number: XTT-C-4b1.

Septomedullopitys Lepekhina, 1972 was first found documented in Russia. *S. szei* Wan et al., 2014 was first described in the Late Permian deposition of Turpan Basin. In the pith of *S. szei*, parenchymatous bands composed of closely arranged brick-like cells are observed. However, these bands are irregularly distributed in the pith, of *S. szei* which is different from the lenses-like diaphragms in the present specimen. Besides, the pith of *S. szei* is septate and heterocellular, long secretory ducts with dark contents being distributed throughout the pith. It differs from the pith of *Turpanopitys* gen. nov., which is solid and lacks secretory ducts.

Phyllocladopitys Kräusel, 1928 was first collected from southwest Africa. It possesses a *Protophyllocladoxylon*-type secondary xylem and homogeneous pith. However, the primary xylem of *Phyllocladopitys* is mesarch or exarch, compared to the endarch primary xylem of *Junggaropitys*.

Medullopitys Kräusel, 1928 and *Megaporoxylon* (Kräusel, 1956) were found in the Early Permian sequences in southwest Africa. They both possess large heterogeneous piths but without diaphragms, contrary to *Turpanopitys* gen. nov.

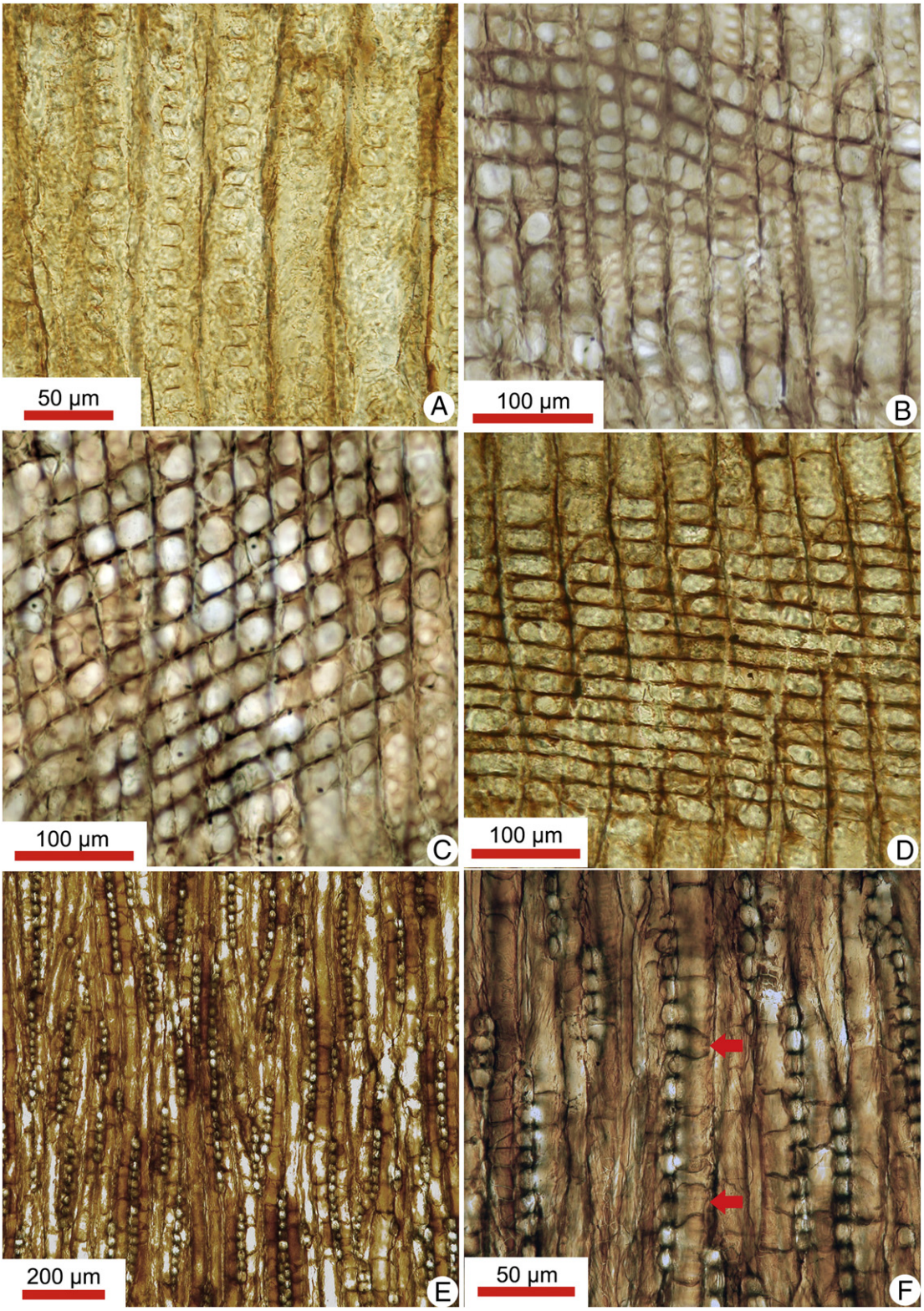

Fig. 7. *Turpanopitys taoshuyuanense* gen. et sp. nov. A. Radial section showing the uniseriate radial pits on the tracheid walls in the main branch. Slide number: XTT-C-4b2. B, C. Radial section showing 1 to 3 rectangular, ovoid or round simple cross-field pits in the branchlet. Slide number: XTT-C-4b1. D. Radial section showing 1 to 3 rectangular, ovoid or round simple cross-field pits in the main branch. Slide number: XTT-C-4b2. E. Tangential section showing the homogeneous, uniseriate or biseriate rays. Slide number: XTT-C-4a1. F. Tangential section showing the homogeneous rays; the red arrows indicate tyloses protruding in the lumen of tracheids. Slide number: XTT-C-4a1. (For interpretation of the references to colour in this figure legend, the reader is referred to the web version of this article.)

Table 1
Comparative features of pith and primary xylem for the species with a *Protophyllocladoxylon*-type secondary xylem.

Genus	Pith	Primary xylem	Type locality and age	References
Turpanopitys gen. nov.	Large, heterogeneous with supporting diaphragms and isodiametric parenchyma cells	Endarch	Xinjiang, China; Early Triassic	The present paper
Phyllocladopitys Kräusel, 1928	Variable, homogeneous with different size of parenchyma cells	Mesarch	South-West Africa; Early Permian. Argentina, South America; early Carboniferous (Pennsylvanian).	Kräusel, 1928; Kräusel et al., 1961; Lepekhina, 1972; Brea and Césari, 1995
Medullopitys Kräusel, 1928	Large, heterogeneous with parenchyma cells and longitudinal sclerenchyma cell strands	Endarch	South-West Africa; Early Permian.	Kräusel, 1928; Kräusel et al., 1961; Lepekhina, 1972
Megaporoxylon Kräusel, 1956	Large, heterogeneous with parenchyma cells and secretory canals	Endarch	South-West Africa and Antarctica; Early Permian.	Kräusel, 1956; Kräusel et al., 1961; Lepekhina, 1972; Maheshwari, 1972;
Septomedullopitys Lepekhina, 1969	Large, septate, heterogeneous with branched secretory canals and irregularly distributed bands	Endarch	Russia and China; Late Permian.	Lepekhina, 1969, 1972; Wan et al., 2014
Junggaropitys Shi et al., 2015	Small, homogeneous with variable sclerenrenchyma cells	Endarch	Xinjiang, China; Middle- Late Triassic.	Shi et al., 2015

Cordaixylon andresii Césari et al., 2015 was documented from Late Pennsylvanian (Stephanian) outcrops at Arnao beach, Spain. It has a *Protophyllocladoxylon*-type secondary xylem, but its pith is homogeneous with isodiametric parenchyma cells and differs from the pith in *Turpanopitys* gen. nov.

Austroscleromedulloxylon (Mussa et al., 1980) was erected as a genus based on samples from the Early Permian of Brazil (Mussa et al., 1980; Mussa, 1986; Crisafulli, 1998). In its pith, the supporting sclerenchymatous diaphragms are present and display a very similar morphology to those of *Turpanopitys* gen. nov. However, the secondary xylem of *Austroscleromedulloxylon* is of *Australoxylon*-type instead of *Protophyllocladoxylon*.

Nandorioxylon saksenae, described by Biradar and Bonde (1981) based on specimens collected from the Late Permian of India, and *Xuanweioxylon* He et al., 2013 was discovered in strata from the Late Permian of South China, display some similarities with those of *Turpanopitys* gen. nov. In the piths of *Nandorioxylon saksenae* and *Xuanweioxylon*, sclerenchymatous sheaths form peripheral annuli in radial direction that is different from the complete diaphragms in *Turpanopitys* gen. nov. Additionally, the secondary xylem of *Nandorioxylon* is also of *Araucarioxylon*-type that is different from *Turpanopitys* gen. nov. *Xuanweioxylon* also contrast with *Turpanopitys* gen. nov., because the tracheids of the latter display scalariform bordered pits.

6. Discussion

6.1. Palaeoecological implications

Growth-ring patterns provide essential information to determine the tree habit (e.g., Falcon-Lang, 2000a, 2000b, 2003; Brea et al., 2008, 2011; Shi et al., 2015). The radial diameter of five adjacent rows of cells were measured to construct the CSDM curve (Fig. 8). We calculated four parameters based on the CSDM curves: (1) skew of CSDM curves, (2) percentage of late wood, (3) percentage of cell diminution in a ring increment and (4) Ring Markedness Index (RMI). (Fig. 9). Deciduous conifers have dominantly left-skewed CSDM or symmetrical curves, whereas evergreen conifers have dominantly right-skewed CSDM curves. The CSDM curves of *Turpanopitys taoshuyuanense* are from +4.92% to +82.41% (mean percentage of skew +38.18%), right-skewed, suggesting that this species was evergreen. This result is consistent with the leaf trace characteristics of *Turpanopitys taoshuyuanense* (see Section 4).

The percentage of late wood in conifer woods could be related to foliar retention (Falcon-Lang, 2000a, 2000b). The late wood development may be strongly influenced by both leaf longevity and the intensity of climate seasonality. The percentage of late wood in *Turpanopitys taoshuyuanense* is 8.79–19.57%, with a mean of 13.66%. The percentage

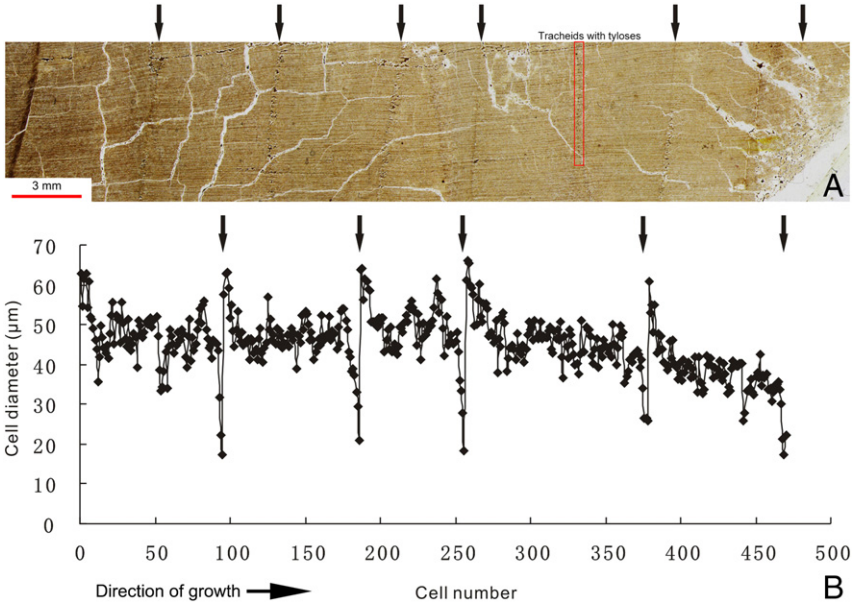

Fig. 8. A. The growth rings with the subtle growth-ring boundary, in the main branch; B. Variation in cell radial diameter across growth rings. Growth is left to right. Arrows indicate the growth-ring boundaries.

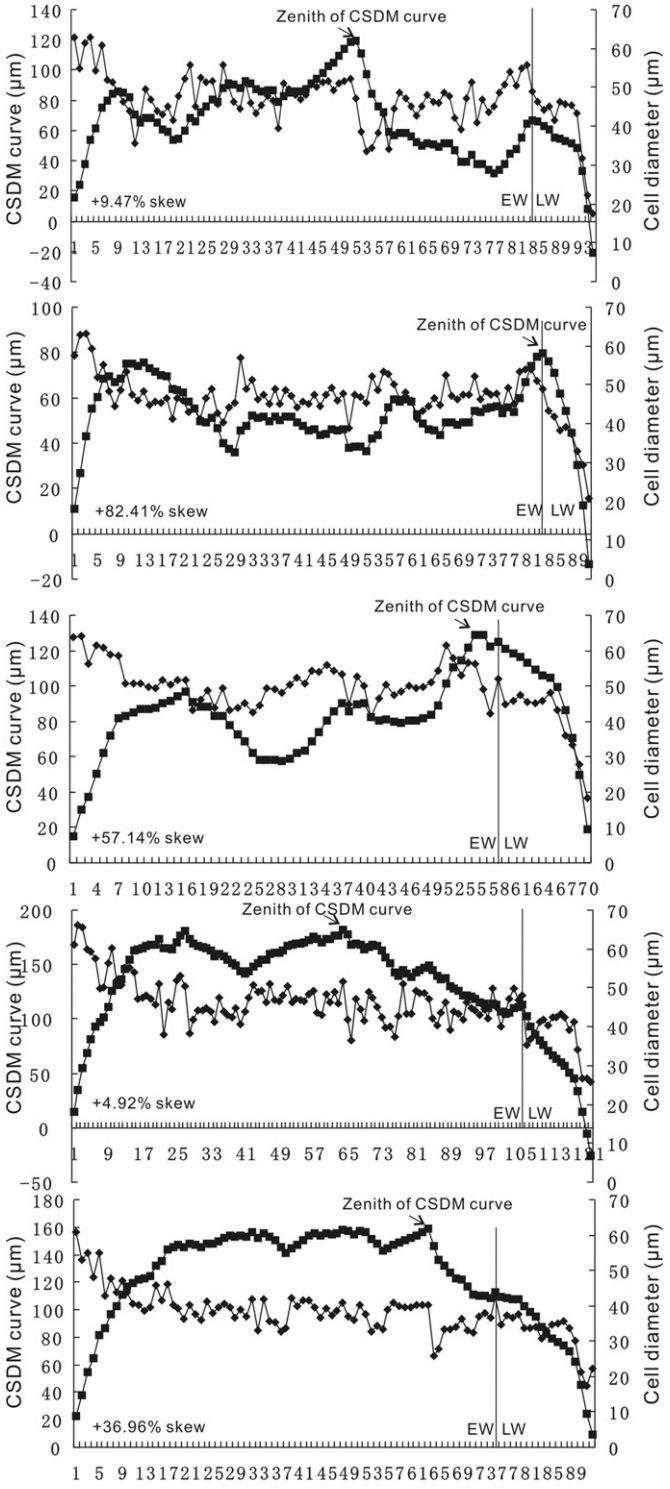

Fig. 9. Right-skewed CSDM curves of five growth rings and cell diameters of growth ring increment. For each ring increment, the percentage of skew for CSDM curves was calculated using Falcon-Lang's (2000a) method. The position at which the CSDM curve reaches the zenith represents the percentage of skew in relation to the total distance between the centres of the CSDM curve to the right of the plot. EW: Early wood, LW Late wood.

of cell diminution ranges from 60.61% to 72.00%, with an average of 73.02%. The RMI varies between 5.86% and 14.12%, with a mean of 9.48% (Table 2). Falcon-Lang (2000a) found a strong inverse linear relationship between the leaf retention and the different quantitative parameters of growth rings (percentage of skew, late wood, cell diminution and RMI values) in the group of extant conifers. The results show that the foliar retention of *Turpanopitys taoshuyuanense* is similar to those of extant conifers with 3–15 years of foliar retention (Table 3).

6.2. Palaeoclimatic conditions

The growth ring analysis is a powerful tool to deduce palaeoclimatic conditions that prevailed during the tree growth (e.g., Schweingruber, 1992, 1996; Falcon-Lang, 2000a, 2000b, 2003; Brea et al., 2008, 2011). The mean radial diameter of five adjacent rows of cells for each growth ring is fluctuant (Fig. 8). Variability in mean cell diameters may result from fluctuations in water supply or other environmental disturbances.

But the factors controlling the formation of growth rings are very complex. Firstly, the growth ring studies must include a taxonomic analysis (Brison et al., 2001). To recognise whether the growth-ring type can indicate the climate conditions, we investigate the palaeobiogeographic distribution of *Protophyllocladoxylon*-type woods in the Palaeozoic and Early Triassic.

Zhang et al. (2010) investigated the distribution of *Protophyllocladoxylon* woods without pith from the Mississipian (Early Carboniferous) to the Palaeogene. Six species of *Protophyllocladoxylon*-type woods were found from the late Palaeozoic (Table 4). The four species described in the southern hemisphere were found in the cool temperate zone. However, *Protophyllocladoxylon*-type woods of the northern hemisphere were found in different climatic zones. Late Permian *P. henanense* (Yao et al., 1994) occurred in the tropical areas, while *P. jingyuanense* (Zhang et al., 2010), from the early Carboniferous North China block, lived in an arid climatic zone.

Ten species belonging to five morphogenera of coniferous fossil woods with a *Protophyllocladoxylon*-type secondary xylem from the late Palaeozoic have been documented (Table 5). All the species found in the southern hemisphere were distributed in the cool temperature zone. (Fig. 10).

Cordaixylon andresii Césari et al., 2015 was documented from late Pennsylvanian Spain. During the Pennsylvanian, Spain was located in the equatorial area. *Protophyllocladoxylon henanense* Yao, Liu and Zhang was found in the Early Permian deposits of North China block, located in the tropical area. This species does not show growth rings as well.

Maheshwari (1972) has investigated the fossil woods from the Permian Antarctica where the climate was cool-temperate (Boucot et al., 2009). He evidenced that *Protophyllocladoxylon dolianitii* Mussa, 1958, *Magaporoxylon antarctium* Maheshwari, 1972 and *Magaporoxylon canalosum* Maheshwari, 1972 all possessed the *Protophyllocladoxylon*-type secondary xylem. The growth-ring types of *M. canalosum* and *M. antarctium* are hard to distinguish in Maheshwari's article. The growth rings of *P. dolianitii* show thick latewood.

Septomedullopitys szei Wan et al., 2014 has been found in the Tarlong area of Turpan Basin in the Late Permian deposits. The climate was considered to be humid climate with short-term, nonperiodic droughts. The growth rings of *S. szei* show a very thin band of latewood.

In consequence, the *Protophyllocladoxylon*-type woods were widely distributed in the southern and northern hemispheres during the Palaeozoic and Early Triassic. The growth rings of the woods with

Table 2
Results of the quantification of ring markedness parameters for *Turpanopitys taoshuyuanense* gen. et sp. nov.

Ring number	Percentage latewood	Percentage diminution	Ring Markedness Index (RMI)	Percentage skews
Ring A	10.5%	73.02%	7.67%	+9.47%
Ring B	8.79%	66.67%	5.86%	+82.41%
Ring C	17.14%	71.88%	12.32%	+57.14%
Ring D	12.30%	60.61%	7.46%	+4.92%
Ring E	19.57%	72.13%	14.12%	+36.96%
Averages	13.66%	68.86%	9.48%	+38.18%

Table 3
Comparison of the quantification of ring markedness parameters for *Turpanopitys taoshuyuanense* gen. et sp. nov. with the five extant taxa taken from the data-base of Falcon-Lang (2000a, 2000b).

Species	Percentage latewood (%)	Percentage diminution (%)	Ring Markedness Index (RMI) (%)	Range of percentage skews (mean value) (%)
Deciduous conifer				
Larix decidua	50.00–54.83	71.55–85.91	35.77–44.36	−40.0 to +7.7 (−6.8)
Evergreen conifers (LRT in years)				
Pinus sylvestris (1–3 years)	41.03–50.00	70.53–77.28	31.56–35.26	−9.1 to +17.9 (+5.2)
Picea abies (3–5 years)	25.93–44.19	74.02–84.03	19.90–35.42	0.0 to +38.2 (+12.0)
Cedrus libani (3–6 years)	30.77–39.58	62.33–72.06	20.22–24.68	+35.7 to +42.9 (+39.0)
***Turpanopitys taoshuyuanense* (? years)**	**8.79–19.57**	**60.61–73.02**	**5.86–14.12**	**+4.92 to + 82.41 (+38.18)**
Araucaria araucana (3–15 years)	10.00–22.50	28.67–51.79	3.17–10.35	+55.0 to +80.0 (66.7)

The bolded species corresponds to the wood fossil studied in this paper.

Table 4
Distribution of morphographic "species" *Protophyllocladoxylon* based only secondary xylem structure during the Palaeozoic.

Species	Type locality and age	Climatic zone	References
Protophyllocladoxylon jingyuanense Zhang et al., 2010	Gansu, China, northern hemisphere; Early Carboniferous.	Arid	Zhang et al., 2010
P. henanense Yao et al., 1994	Henan, China, northern hemisphere; Early Permian.	Tropical	Yao et al., 1994
P. dolianitii Mussa, 1958	Brazil, southern hemisphere; Late Carboniferous.	Cool temperate	Mussa, 1958
P. derbyi (Oliveira) Maheshwari, 1972	Brazil, southern hemisphere; Late Carboniferous/Early Permian.	Cool temperate	Maheshwari, 1972
P. indicum Pant and Singh, 1987	India, southern hemisphere; Late Permian	Cool temperate	Pant and Singh, 1987
P. natalense (Warren) Schultze-Motel, 1961	South Africa, southern hemisphere; Early Permian	Cool temperate	Schultze-Motel, 1961

Table 5
Distribution of the species with *Protophyllocladoxylon*-type secondary xylem during the Palaeozoic.

Species	Type locality and age	Climatic zone	References
Turpanopitys taoshuyuanense gen. et nov. sp.	Xinjiang, China, northern hemisphere; Early Triassic	Warm temperate	The present paper
Septomedullopitys sibirica Lepekhina, 1969	Kuznetsk Basin, Russia, northern hemisphere; Late Permian.	Warm temperate	Lepekhina, 1969, 1972
Septomedullopitys szei Wan et al., 2014	Xinjiang, China, northern hemisphere; Late Permian	Warm temperate	Wan et al., 2014
Cordaixylon andresii Césari et al., 2015	Spain, equator; Stephanian, Late Carboniferous	Tropical	Césari et al., 2015
Phyllocladopitys petriellae Brea and Césari, 1995	Argentina, southern hemisphere; early Late Carboniferous	Cool temperate	Brea and Césari, 1995
Medullopitys menendezii Petriella, 1982	Argentina, southern hemisphere; Late Carboniferous	Cool temperate	Petriella, 1982
Phyllocladopitys capensis Kräusel, 1928	South-West Africa, southern hemisphere; Early Permian.	Cool temperate	Kräusel, 1928; Kräusel et al., 1961; Lepekhina, 1972
Megaporoxylon kaokense Kräusel, 1956	South-West Africa, southern hemisphere; Early Permian	Cool temperate	Kräusel, 1956; Kräusel et al., 1961; Lepekhina, 1972
Medullopitys sclerotic Kräusel, 1928	South-West Africa, southern hemisphere; Early Permian.	Cool temperate	Kräusel, 1928; Kräusel et al., 1961; Lepekhina, 1972
Megaporoxylon canalosum Maheshwari, 1972	Antarctica, southern hemisphere; Middle/Late Permian	Cool temperate	Maheshwari, 1972
Megaporoxylon antarcticum Maheshwari, 1972	Antarctica, southern hemisphere; Middle/Late Permian	Cold/cool temperate	Maheshwari, 1972

Protophyllocladoxylon-type secondary xylem can be used as indicator of palaeoclimate.

The species was evergreen. Thus, the leaf abscission is not the reason for the growth-ring formation. Growth rings displaying subtle ring boundaries are related to weakly developed climate seasonality (Falcon-Lang, 1999). During the Late Permian to Early Triassic, palaeoclimatic reconstruction shows a temperate climate in this area (e.g., Kiehl and Shields, 2005; Péron et al., 2005; Boucot et al., 2009), in accordance with the mean annual temperature of 7–15 (±4.4) °C estimated from palaeosols proxies from the Turpan Basin (Thomas et al., 2011). Consequently, the growth rings of *Turpanopitys taoshuyuanense* do not appear to be related to these relatively moderate annual temperature ranges. On the contrary, Late Permian to Early Triassic palaeosoils from the Turpan Basin display features indicative of variable soil moisture regimes (Thomas et al., 2011). Thus, we speculate that dry episodes trigged the formation of growth rings. Moreover, the width of growth rings ranges from 3.8 mm to 8.4 mm. Variability in mean cell diameters may result from fluctuations in water supply or other environmental disturbances (Fig. 8). It indicates that the growing environment was not uniform. In conclusion, *Turpanopitys taoshuyuanense* developed under a mainly warm humid climate condition with short dry periods or of hydric stresses due to the irregularity of water supplies.

7. Conclusions

The genus *Turpanopitys* gen. nov. is discovered for the first time in the Early Triassic deposits of the Turpan Basin. This genus displays diaphragms in the pith, a unique characteristic that distinguish it from any other species with *Protophyllocladoxylon*-type wood reported up to now. The presence of diaphragms within the pith plays a supportive role. The quantitative growth-ring analysis allows hypothesizing that *T. taoshuyuanense* was an evergreen gymnosperm, the foliar retention being probably of 3–15 years. Morphometric characteristics displayed by *T. taoshuyuanense* indicates it developed under irregularly stressed warm-temperate conditions.

The discovery of the new genus *Turpanopitys* gen. nov. in the Guodikeng Formation of the Turpan basin contributes to a better understanding of the plant diversity during Permian-Triassic transition. Wang (1996) described the process of vegetation recovery from the end Permian mass extinction in North China. He pointed out that the vegetation

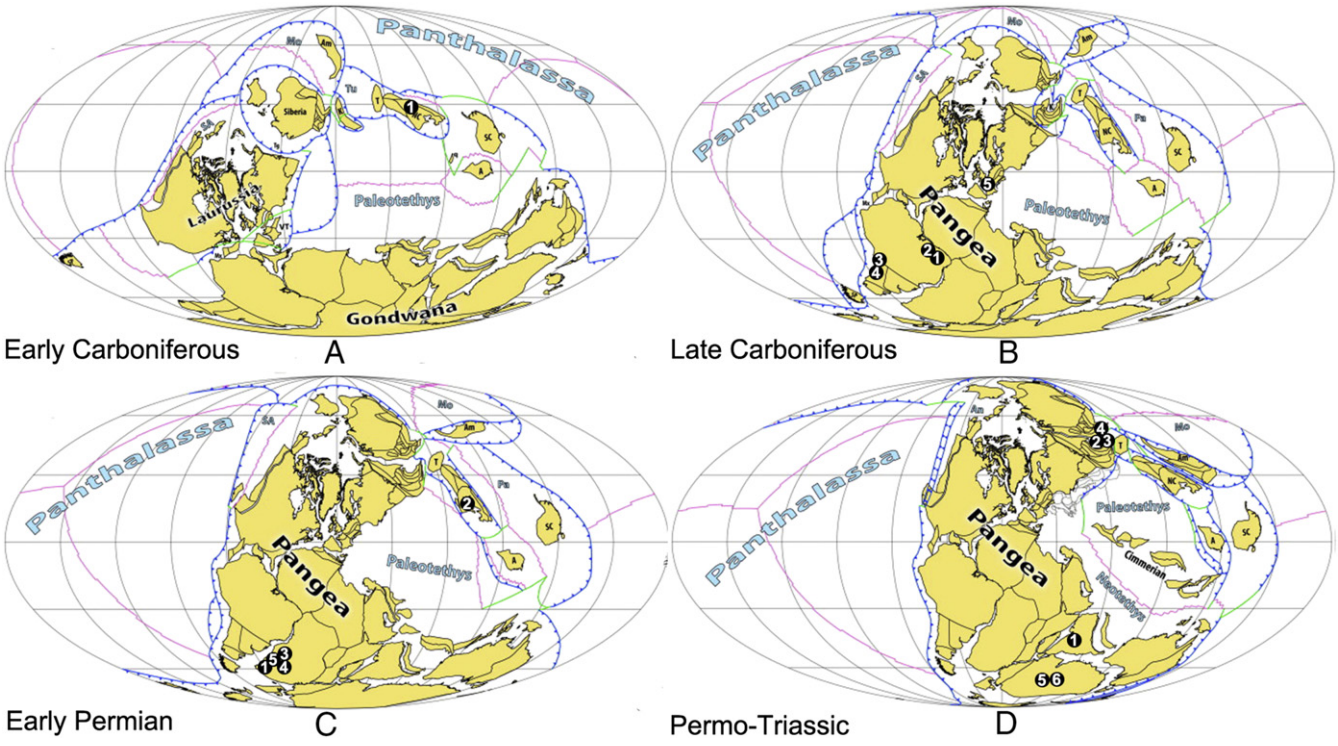

Fig. 10. Distribution of the woods with *Protophyllocladoxylon*-type secondary xylem during the Palaeozoic. A. 1. *Protophyllocladoxylon jingyuanense* B. 1. *Protophyllocladoxylon dolianitii*; 2. *P. derbyi*; 3. *Medullopitys menendezii*; 4. *Phyllocladopitys petriellae*; 5. *Cordaixylon andresii*. C. 1. *Protophyllocladoxylon natalense*; 2. *P. henanense*; 3. *Phyllocladopitys capensis*; 4. *Megaporoxylon kaokense*; 5. *Medullopitys sclerotic*. D. 1. *Protophyllocladoxylon indicum*; 2. *Turpanopitys taoshuyuanense*; 3. *Septomedullopitys szei*; 4. *Septomedullopitys sibirica*; 5. *Megaporoxylon canalosum*; 6. *M. antarcticum*.

recovery was completed in the latest Middle Triassic. For the Turpan Basin, abundant conifer fossil woods were found in the early Early Triassic sequences. Looy et al. (1999) noted that in most locations the floral recovery was associated with the re-establishment of coniferous forests. These new discoveries are in good agreement with the Looy et al. statement. The occurrence of *Turpanopitys taoshuyuanense* gen. et sp. nov. might indicate a warm humid climate with irregularly distributed short dry periods and Palaeo-Tethys megamonsoons did not influence the Turpan basin long the east coast of mid-latitude Pangaea in the Early Triassic. We hope to find more evidences (e.g. palynological data, sedimentological data and organic geochemistry data) to know more about the biodiversity and the climatic conditions of that period.

Acknowledgments

The authors are thankful to Prof. Wu Zhang and Prof. Shaolin Zheng of Shenyang Institute of Geology and Mineral Resources and Anais Boura of Pierre et Marie Curie University for their help in identifying the fossil woods and providing relevant materials. We thank Dr. Daoliang Chu and Mr. Wei Zhang of China University of Geosciences for collecting the sample. We also thank two anonymous reviewers for extremely helpful feedback and constructive comment on the article. The study was supported by National Natural Science Foundation of China (Grant No. 41572005, 41272024).

References

Allen, M.B., Sengor, A.M.C., Natal'in, B.A., 1995. Junggar, Turfan and Alakol basins as Late Permian to ?Early Triassic extensional structures in a sinistral shear zone in the Altaid orogenic collage, Central Asia. J. Geol. Soc. 152 (2), 327–338.

Benton, M.J., Newell, A.J., 2014. Impacts of global warming on Permo-Triassic terrestrial ecosystems. Gondwana Res. 25 (4), 1308–1337.

Biradar, N.V., Bonde, S.D., 1981. *Nandorioxylon saksenae* gen. et sp. nov. — a new gymnospermous wood from the Kamthi Stage of Chandrapur District, Maharashtra State, India. Geophytology 11, 90–95.

Boucot, A.J., Chen, X., Scotese, C.R., Fan, J.X., 2009. Phanerozoic Global Climatic Reconstruction. Science Press, Beijing (173 pp. (In Chinese)).

Brea, M., Césari, S.N., 1995. An anatomically preserved stem from the carboniferous of Gondwana: *Phyllocladopitys petriellae* Brea and Césari, sp. nov. Rev. Palaeobot. Palynol. 86 (3), 315–323.

Brea, M., Artabe, A., Spalletti, L.A., 2008. Ecological reconstruction of a mixed Middle Triassic forest from Argentina. Alcheringa 32 (4), 365–393.

Brea, M., Matheos, S.D., Raigemborn, M.S., Iglesias, A., Zucol, A.F., Prámparo, M.B., 2011. Paleoecology and paleoenvironments of Podocarp trees in the Ameghino Petrified forest (Golfo San Jorge Basin, Patagonia, Argentina): constraints for early Paleogene paleoclimate. Geol. Acta 9 (1), 13–28.

Brison, A.L., Philippe, M., Thevenard, F., 2001. Are Mesozoic wood growth rings climate-induced? Palaeobiology 27, 531–538.

Cao, C., Wang, W., Liu, L., Shen, S., Summons, R.E., 2008. Two episodes of ^{13}C depletion in organic carbon in the latest Permian: evidence from the terrestrial sequences in northern Xinjiang, China. J. Asian Earth Sci. 270 (34), 251–257.

Cascales-Miñana, B., Cleal, C.J., 2013. The plant fossil record reflects just two great extinction events. Terra Nova 26 (3), 195–200.

Césari, S.N., Álvarez-Vázquez, C., Méndez-Bedia, I., Álvarez-Laó, D., Turrero, P., Arbizu, M., 2015. First report of permineralised plants in the Stephanian of Arnao (Asturias, northwestern Spain). Palaeogeogr. Palaeoclimatol. Palaeoecol. 440, 475–486.

Chen, Z.Q., Benton, M.J., 2012. The timing and pattern of biotic recovery following the end-Permian mass extinction. Nat. Geosci. 5 (6), 375–383.

Cheng, Z.W., Wu, S.Z., Fang, X.S., 1996. The Permian–Triassic sequences in the southern margin of the Junggar Basin and the Turpan Basin, Xinjiang, China. In: Hongfei, H., Jinsong, Z. (Eds.), Field Trip Guide, Volume 1, Stratigraphy, Paleontology, Sedimentology, Petroleum and Coal Geology30th International Geological Congress. Geological Publishing House, Beijing, China.

Crisafulli, A., 1998. Leños gimnospérmicos de la Formación Melo (Pérmico inferior), Uruguay. Parte II. *Stiloxylon*, *Polysolenoxylon* y *Bageopitys*. Ameghiniana 35 (2), 133–140.

Domeier, M., Torsvik, T.H., 2014. Plate tectonics in the late Paleozoic. Geosci. Front. 5: 303–350. http://dx.doi.org/10.1016/j.gsf.2014.01.002.

Falcon-Lang, H.J., 1999. The early carboniferous (Courceyan–Arundian) monsoonal climate of the British Isles. Geol. Mag. 136, 177–187.

Falcon-Lang, H.J., 2000a. A method to distinguish between woods produced by evergreen and deciduous coniferopsids on the basis of growth ring anatomy: a new palaeoecological tool. Palaeontology 43 (4), 785–793.

Falcon-Lang, H.J., 2000b. The relationship between leaf longevity and growth ring markedness in modern conifer woods and its implications for palaeoclimatic studies. Palaeogeogr. Palaeoclimatol. Palaeoecol. 160 (3), 317–328.

Falcon-Lang, H.J., Cantrill, D.J., 2001. Leaf phenology of some mid-Cretaceous polar forests, Alexander Island, Antarctica. Geol. Mag. 138 (1), 39–52.

Falcon-Lang, H.J., 2003. Growth interruptions in silicified conifer woods from the Upper Cretaceous Two Medicine Formation, Montana, USA: implications for palaeoclimate and dinosaur. Palaeogeogr. Palaeoclimatol. Palaeoecol. 199 (3), 299–314.
Falcon-Lang, H.J., Kurzawe, F., Lucas, S.G., 2014. Coniferopsid tree trunks preserved in sabkha facies in the Permian (Sakmarian) Community Pit Formation in south-central New Mexico, USA: systematics and palaeoecology. Rev. Palaeobot. Palynol. 200, 138–160.
Falcon-Lang, H.J., Kurzawe, F., Lucas, S.G., 2016. A Late Pennsylvanian coniferopsid forest in growth position, near Socorro, New Mexico, USA: tree systematics and palaeoclimatic significance. Rev. Palaeobot. Palynol. 225, 67–83.
Feng, Z., Wang, J., Rößler, R., 2011. A unique gymnosperm from the latest Permian of China, and its ecophysiological implications. Rev. Palaeobot. Palynol. 165 (1), 27–40.
Greene, T.J., Carroll, A.R., Wartes, M., Graham, S.A., Wooden, J.L., 2005. Integrated provenance analysis of a complex orogenic terrane: Mesozoic uplift of the Bogda Shan and inception of the Turpan-Hami Basin, NW China. J. Sediment. Res. 75:251–267. http://dx.doi.org/10.2110/jsr.2005.019.
Hernandez-Castillo, G.R., Stockey, R.A., Rothwell, G.W., Mapes, G., 2009a. A new voltzialean conifer, *Emporia royalii* sp. nov. (Emporiaceae) from the Hamilton Quarry, Kansas. Int. J. Plant Sci. 170, 1201–1227.
Hernandez-Castillo, G.R., Stockey, R.A., Rothwell, G.W., Mapes, G., 2009b. Whole plant reconstruction of *Emporia lockardii* (Emporiaceae) Voltziales and initial thoughts on Paleozoic conifer ecology. Int. J. Plant Sci. 170, 1056–1074.
Hernandez-Castillo, G.R., Stockey, R.A., Rothwell, G.W., Mapes, G., 2009c. Reconstruction of the Pennsylvanian-aged walchia conifer, *Emporia cryptica* sp. nov. (Emporiaceae, Voltziales). Rev. Palaeobot. Palynol. 157, 218–237.
Jablonski, D., 1985. Extinctions in the fossil record. Philos. Trans.: Biol. Sci. 344 (1307), 11–16.
Kiehl, J.T., Shields, C.A., 2005. Climate simulation of the latest Permian: implications for mass extinction. Geology 33:757–760. http://dx.doi.org/10.1130/G21654.1.
Knoll, A.H., Bambach, R.K., Payne, J.L., Pruss, S., Fischer, W.W., 2007. Paleophysiology and end-Permian mass extinction. Earth Planet. Sci. Lett. 256:295–313. http://dx.doi.org/10.1016/j.epsl.2007.02.018.
Kräusel, R., 1928. Paläobotanische Notizen, X. Über ein Keuperholz mit cordaitem Mark. Senckenbergiana Lethaia 10, 247–250.
Kräusel, R., 1956. Hölzer aus dem Südlichen Gebiet der Karru-Schichten Südwest-Afrikas. Senckenb. Lethaea 37, 447–453.
Kräusel, R., Maithy, P.K., Maheshwari, H.K., 1961. Gymnospermous woods with primary structures from Gondwana rocks-a review. The Palaeobotanist 10, 97–107.
Lepekhina, V.G., 1969. Paleoxylological characterization of the Upper Palaeozoic coal-bearing deposits of the Kuznetsk Basin. Translation Geological Institute Academy of Sciences USSR 130, 126–140 (In Russian).
Lepekhina, V.G., 1972. Woods of Palaeozoic pycnoxylic gymnosperms with special reference to North Eurasia representatives. Palaeontogr. Abt. B 138 (1–4), 44–106.
Li, Y., Li, J., Cheng, Z., Sun, D., Liu, J., Zheng, J., 2004. Study on paleomagnetism of Permian-Trassic in Pantaoyuan of Turpan, Xinjiang. Xinjiang Geol. 22 (2), 136–142 (In Chinese with English abstract).
Liao, Z., Lu, L., Jiang, N., Xia, F., Song, F., Zhou, Y., Li, S., Zhang, Z., 1987. Carboniferous and Permian in the western part of the east Tianshan Mountains. Eleventh Congress of Carboniferous Stratigraphy and Geology, Guidebook Excursion 4. Beijing, China (50 pp).
Liu, Z., 2000. The Peimian-Triassic boundary on the northern margin of the Turpan-Hami Basin of Xinjiang, NW China. J. Stratigr. 24 (4), 310–314 (In Chinese with English abstract).
Looy, C.V., Brugman, W.A., Dilcher, D.L., Visscher, H., 1999. The delayed resurgence of equatorial forests after the Permian–Triassic ecologic crisis. Proc. Natl. Acad. Sci. 96 (24), 13857–13862.
Lucas, S.G., 1998. Global Triassic tetrapod biostratigraphy and biochronology. Palaeogeogr. Palaeoclimatol. Palaeoecol. 143:347–384. http://dx.doi.org/10.1016/S0031-0182(98)00117-5.
Lucas, S.G., 2009. Timing and magnitude of tetrapod extinctions across the Permo-Triassic boundary. J. Asian Earth Sci. 36:491–502. http://dx.doi.org/10.1016/j.jseaes.2008.11.016.
Maheshwari, H.K., 1972. Permian wood from Antarctica and revision of some Lower Gondwana wood taxa. Palaeontogr. Abt. B 138, 1–43.
Metcalfe, I., Foster, C.B., Afonin, S.A., Nicoll, R.S., Mundil, R., Wang, X., Lucas, S.G., 2009. Stratigraphy, biostratigraphy and C-isotopes of the Permian–Triassic non-marine sequence at Dalongkou and Lucaogou, Xinjiang Province, China. J. Asian Earth Sci. 36: 503–520. http://dx.doi.org/10.1016/j.jseaes.2008.06.005.
McElhinny, M.W., Embleton, B.J.J., Ma, X.H., Zhang, Z.K., 1981. Fragmentation of Asia in the Permian. Nature 293, 212–216.
Mussa, D., 1958. Conifera fóssil do carbonifero superior de Santa Catarina. 182. Boletim Departamento Nacional da Produção Mineral, Divisão de Geologia e Mineralogia, pp. 1–23.
Mussa, D., de Carvalho, R.G., dos Santos, P.R., 1980. Estudo estratigráfico e paleoecológico em ocorrências fossilíferas da Formação Irati, Estado de São Paulo, Brasil. 1. Boletim IG-USP Instituto de Geociências da Universidade de São Paulo, pp. 142–149.
Mussa, D., 1986. Eustelos Gondwanicos de medullas diafragmadas e a sua posicão estratigrafica. 17. Boletim IG-USP Instituto de Geociências da Universidade de São Paulo, pp. 11–26.
Pant, D.D., Singh, V.K., 1987. Xylotomy of some woods from Raniganj Formation (Permian), Raniganj Coalfield, India. Palaeontogr. Abt. B 203, 1–82.
Péron, S., Bourquin, S., Fluteau, F., Guillocheau, F., 2005. Paleoenvironment reconstructions and climate simulations of the Early Triassic: impact of the water and sediment supply on the preservation of fluvial systems. Geodin. Acta 18, 431–446.
Petriella, B., 1982. *Medullopitys menendezii* n. sp., leño picnoxilico de gimnospermas del Paleozóico Superior de Mendoza. Argentina. Ameghiniana 19 (3/4), 253–257.
Retallack, G.J., Sheldon, N.D., Carr, P.F., Fanning, M., Thompson, C.A., Williams, M.L., Jones, B.G., Hutton, A., 2011. Multiple Early Triassic greenhouse crises impeded recovery from Late Permian mass extinction. Palaeogeogr. Palaeoclimatol. Palaeoecol. 308 (1), 233–251.
Retallack, G.J., 2013. Permian and Triassic greenhouse crises. Gondwana Res. 24, 90–103.
Rothwell, G.W., Mapes, G., 2001. *Barthelia furcata* gen. et sp. nov., with review of Paleozoic coniferophytes and discussion of coniferophyte systematics. Int. J. Plant Sci. 162, 637–667.
Rothwell, G.W., Mapes, G., Hernandez-Castillo, G.R., 2005. *Hanskerpia* gen. nov. and phylogenetic relationships among the most ancient conifers (Voltziales). Taxon 54, 733–750.
Royer, D.L., Wilf, P., Janesko, D., Kowalski, E., Dilcher, D., 2005. Correlations of climate and plant ecology to leaf size and shape: potential proxies for the fossil record. Am. J. Bot. 92:1141–1151. http://dx.doi.org/10.3732/ajb.92.7.1141.
Sengor, A.M.C., Nat'lin, B.A., 1996. Paleotectonics of Asia: fragments of a synthesis. In: Yin, A., Harrison, T.M. (Eds.), The Tectonic Evolution of Asia. Cambridge University Press, New York, pp. 486–640.
Schweingruber, F.H., 1992. Annual growth rings and growth zones in woody plants in southern Australia. IAWA Bulletin 13, 359–379.
Schweingruber, F.H., 1996. Tree Rings and Environment Dendroecology. Swiss Federal Institute for Forest, Berne, pp. 1–609.
Schultze-Motel, J., 1961. Gymnospermen-Hölzer aus dem Jura des Nördlichen Harzvorlandes: *Protophyllocladoxylon quedlinburgense* n. sp. Mber. Dtsch. Akad. Wiss 3, 418–426.
Scotese, C.R., 2001. Atlas of Earth History. 1. PALEOMAP Project, Arlington, Texas.
Shi, X., Yu, J., Broutin, J., Pons, D., 2015. *Junggaropitys*, a new gymnosperm stem from the Middle–Late Triassic of Junggar Basin, Northwest China, and its palaeoecological and palaeoclimatic implications. Rev. Palaeobot. Palynol. 223, 10–20.
Smith, R.M.H., Ward, P.D., 2001. Pattern of vertebrate extinctions across an event bed at the Permian-Triassic boundary in the Karoo Basin of South Africa. Geology 29: 1147–1150. http://dx.doi.org/10.1130/0091-7613(2001)029<1147:POVEAA>2.0.CO;2.
Sun, F., 1989. On the Late Permian Angara flora of Turfan Basin, Xinjiang, with Special Reference to the Subdivision of Angara Province. -M.Sc. thesis. Nanjing Institute of Geology and Palaeontology, Chinese Academy of Sciences, pp. 1–192 (in Chinese with English abstract).
Sun, Y., Joachimski, M.M., Wignall, P.B., Yan, C., Chen, Y., Jiang, H., Wang, L., Lai, X., 2012. Lethally hot temperatures during the Early Triassic greenhouse. Science 338 (6105), 366–370.
Thomas, S.G., Tabor, N.J., Yang, W., Myers, T.S., Yang, Y., Wang, D., 2011. Palaeosol stratigraphy across the Permian–Triassic boundary, Bogda Mountains, NW China: implications for palaeoenvironmental transition through earth's largest mass extinction. Palaeogeogr. Palaeoclimatol. Palaeoecol. 308 (1–2), 41–64.
Twitchett, R.J., Looy, C.V., Morante, R., Visscher, H., Wignall, P.B., 2001. Rapid and synchronous collapse of marine and terrestrial ecosystems during the end-Permian biotic crisis. Geology 29:351. http://dx.doi.org/10.1130/0091-7613(2001)029<0351:RASCOM>2.0.CO;2.
Wan, M., Yang, W., Wang, J., 2014. *Septomedullopitys szei* sp. nov., a new gymnospermous wood from Lower Wuchiapingian (Upper Permian) continental deposits of NW China, and its implication for a weakly seasonal humid climate in mid-latitude NE Pangaea. Palaeogeogr. Palaeoclimatol. Palaeoecol. 407 (1), 1–13.
Wang, Z.Q., 1996. Recovery of vegetation from the terminal Permian mass extinction in North China. Rev. Palaeobot. Palynol. 91 (1), 121–142.
Wang, Z.Q., Zhang, Z.P., 1998. Gymnosperms on the eve of the terminal Permian mass extinction in North China and their survival strategies. Chin. Sci. Bull. 43 (11), 889–897.
Wartes, M.A., Carroll, A.R., Greene, T.J., 2002. Permian sedimentary record of the Turpan–Hami Basin and adjacent regions, Northwest China; constraints on postamalgamation tectonic evolution. Geol. Soc. Am. Bull. 114, 131–152.
Xiao, W., Kröner, A., Windley, B.F., 2009. Geodynamic evolution of Central Asia in the Paleozoic and Mesozoic. Int. J. Earth Sci. 98:1185–1188. http://dx.doi.org/10.1007/s00531-009-0418-4.
He, J., Wang, S.J., Hilton, J., Shao, L., 2013. *Xuanweioxylon scalariforme* gen. et sp. nov.: novel Permian coniferophyte stems with scalariform bordered pitting on secondary xylem tracheids. Rev. Palaeobot. Palynol. 197, 152–165.
Yang, W., Liu, Y., Feng, Q., Lin, J., Zhou, D., Wang, D., 2007. Sedimentary evidence of Early–Late Permian mid-latitude continental climate variability, southern Bogda Mountains, NW China. Palaeogeogr. Palaeoclimatol. Palaeoecol. 252, 239–258.
Yang, W., Feng, Q., Liu, Y., Tabor, N., Miggins, D., Crowley, J.L., Lin, J., Thomas, S., 2010. Depositional environments and cyclo- and chronostratigraphy of uppermost carboniferous–Lower Triassic fluvial–lacustrine deposits, southern Bogda Mountains, NW China – a terrestrial palaeoclimatic record of mid-latitude NE Pangea. Glob. Planet. Chang. 73, 15–113.
Yao, Z.Q., Liu, L.J., Zhang, S., 1994. Permian wood from western Henan, China: implications for palaeoclimatological interpretations. Rev. Palaeobot. Palynol. 80 (3), 277–290.
Zhang, X., 1981. Regional Stratigraphic Chart of Northwestern China, Branch of Xinjiang Uygur Autonomous Region. Geological Publishing House, Beijing (496 pp. (in Chinese)).
Zhang, Y., Wang, J., Liu, L., Li, N., 2010. *Protophyllocladoxylon jingyuanense* sp. nov., a gymnospermous wood of the Serpukhovian (Late Mississippian) from Gansu, Northwest China. Acta Geol. Sin. 84, 257–268.
Ziegler, A.M., Hulver, M.L., Rowley, D.B., 1997. Permian world topography and climate. In: Martini, I.P. (Ed.), Late Glacial and Postglacial Environmental Changes: Pleistocene, Carboniferous–Permian, and Proterozoic. Oxford University Press, Oxford, pp. 111–146.
Zhu, H.C., Ouyang, S., Zhan, J.Z., Wang, Z., 2005. Comparison of Permian palynological assemblages from the Junggar and Tarim basins and their phytoprovincial significance. Rev. Palaeobot. Palynol. 136, 181–207.